ANTIOXIDANTS & REDOX SIGNALING
Volume 3, Number 4, 2001
Mary Ann Liebert, Inc.

Forum Original Research Communication

Role of Zinc-Finger Motif in Redox Regulation of Human Replication Protein A

MU WANG, JIN-SAM YOU, and SUK-HEE LEE

ABSTRACT

Replication protein A (RPA) is a heterotrimeric zinc-finger protein complex involved in DNA replication, repair, and genetic recombination. Unlike other zinc-finger proteins, RPA's zinc-finger motif is not essential for its single-stranded DNA (ssDNA) binding activity, but is involved in redox regulation of its single-stranded DNA (ssDNA) binding activity. To get an insight into the regulation of RPA–ssDNA interaction, wild-type RPA (wt-RPA) and zinc-finger mutant were examined for ssDNA binding activity using surface plasmon resonance technique. Interaction of wt-RPA with ssDNA under nonreducing conditions was very weak ($K_D \times 2.33 \times 10^{-8}$ *M*) compared with that under reducing conditions ($K_D = 7.35 \times 10^{-11}$ *M*), whereas ssDNA binding affinity of the zinc-finger mutant was not affected by redox. The divalent ion chelator, *o*-phenanthroline, significantly reduced wt-RPA–ssDNA interaction, but had no effect on the zinc-finger mutant. The inhibitory effect of *o*-phenanthroline on RPA–ssDNA interaction was reversed by Zn(II), but not by other divalent cations, suggesting that Zn(II) is the unique metal coordinating the zinc-finger cysteines in redox regulation of RPA–ssDNA interaction. In DNA repair, redox affected RPA's interaction with damaged DNA, but not its role in stabilizing the xeroderma pigmentosum group A (XPA)-damaged DNA complex, suggesting that the zinc-finger motif may mediate the transition of RPA–XPA interaction to a stable RPA–XPA-damaged DNA complex in a redox-dependent manner. Antioxid. Redox Signal. 3, 657–669.

INTRODUCTION

REPLICATION PROTEIN A [RPA; also known as human single-stranded DNA (ssDNA) binding protein, HSSB] is a three-subunit protein complex consisting of 70-, 34-, and 11-kDa subunits involved in DNA replication, repair, and genetic recombination (Fig. 1A) (28). In DNA replication, RPA is involved in unwinding of the replication origin, whereas it interacts with the DNA polymerase α-primase complex at the origin (5, 7, 15, 20). In nucleotide excision repair (NER), RPA interacts with the xeroderma pigmentosum group A complementing protein (XPA) on damaged DNA and stimulates XPA–DNA interaction and also recruits other repair proteins such as XPG, excision repair cross complementing protein 1 (ERCC1)-XPF, and transcription factor IIH (TFIIH) to the damaged site for the subsequent incision/excision step (11, 19). RPA may also be involved in a later stage of NER, gap-filling, that requires PCNA, RF-C, and DNA polymerase δ (or ε) (1).

The large subunit of RPA (p70) contains the ssDNA-binding domain that resides in the middle region of p70 with two homologous subdomains in tandem positions (3, 8, 14, 16). RPA p70 has a 4-cysteine type zinc-finger motif toward the C-terminus (amino acids

Department of Biochemistry and Molecular Biology, Indiana University Cancer Center and Walther Oncology Center, Indiana University School of Medicine, Indianapolis, IN 46202.

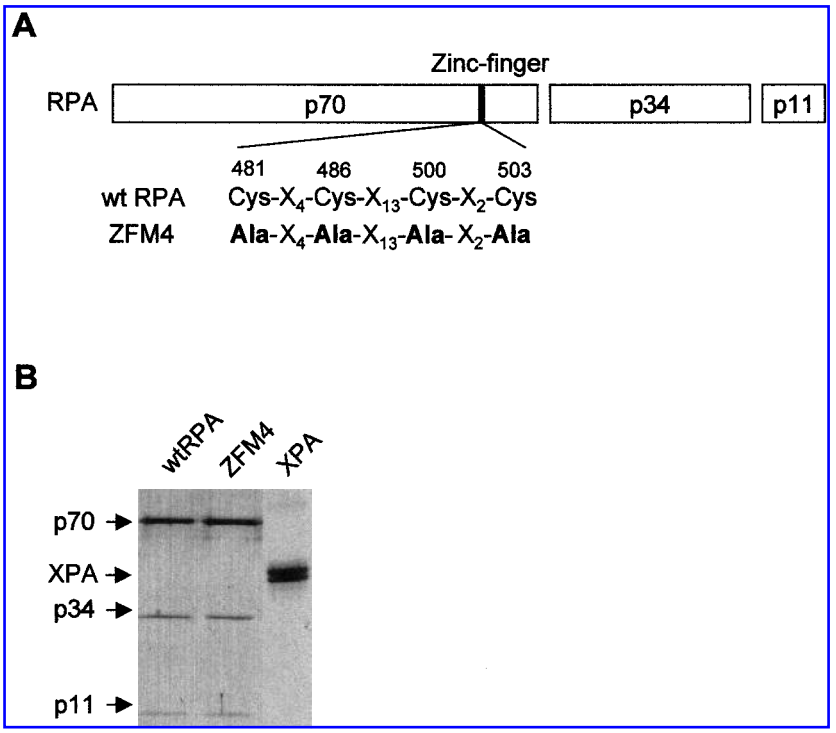

FIG. 1. Proteins used for this study. (**A**) Schematic representation of wild-type RPA (wt-RPA) and a zinc-finger mutant RPA [ZFM4; containing cysteine-to-alanine substitution at all four cysteine sites (amino acids 481, 486, 500, and 503)]. (**B**) SDS-PAGE of purified proteins. Proteins were separated by 12% SDS-PAGE followed by Coomassie Blue staining (see Materials and Methods).

481–503; Fig. 1A) (21, 30). Unlike other zinc-finger proteins, RPA's zinc-finger domain is not essential for its ssDNA binding activity and has little or no effect on its DNA binding activity (14, 16). Recent studies have shown that RPA's ssDNA binding activity is regulated by redox through the cysteines in a putative zinc-finger domain (21, 30). In fact, all four zinc-finger cysteines are required for redox regulation of RPA's DNA binding activity (30). Under reduced condition, the zinc-finger structure is favorably formed and Zn(II) may protect the zinc-finger cysteines from engaging in disulfide bond formation. Under nonreducing conditions, however, oxidation of the Zn(II)-thiolate bond induces the release of Zn(II) from the pocket (21), which promotes the formation of disulfide bonds (21, 30). The redox status of RPA significantly affected initial interaction with ssDNA, but had no effect after RPA formed a stable complex with DNA (30), suggesting that redox regulation of the zinc finger may be involved in mediating initial RPA–ssDNA interaction to form a stable RPA–ssDNA complex.

XPA is also a zinc-finger protein involved in the damage recognition step of NER (10, 13, 24). XPA preferentially binds to (6-4) photoproduct of ultraviolet ray (UV)-damaged DNA and may also play a role in subsequent steps of NER through interaction with other repair proteins (13). XPA exhibits a low-affinity binding to UV-damaged DNA; hence, the interaction between XPA and RPA stimulates the XPA-damaged DNA complex and also recruits other repair proteins such as XPG, ERCC1-XPF, and TFIIH to the damaged site for the subsequent incision/excision step (11, 19, 27). A mutation of RPA at any zinc-finger cysteine abolished its function in repair (6), suggesting a unique role for the zinc-finger domain in the early stage of repair.

To understand the role of the zinc-finger motif in the redox regulation of RPA–DNA interaction, we carried out a real-time analysis of

the interaction between RPA (and XPA) and DNA using the surface plasmon resonance (SPR) technique. We found that interaction of wild-type RPA (wt-RPA) with ssDNA under nonreducing conditions was 1/3,000th of the affinity observed under reducing conditions, whereas the zinc-finger mutant exhibited a strong binding to ssDNA regardless of its redox status. RPA-damaged DNA interaction was also regulated by redox, although RPA's role in stabilization of the XPA-damaged DNA complex was not affected by redox, suggesting that the zinc-finger motif may mediate the transition of RPA–XPA interaction to a stable RPA–XPA-damaged DNA complex in a redox-dependent manner.

MATERIALS AND METHODS

Proteins and antibodies

wt-RPA and a zinc-finger mutant [ZFM4; the mutation with the change of all four cysteines (the sites 481, 486, 500, and 503) into alanines] were prepared according to the procedure described previously with slight modifications (6). In brief, cell lysates were prepared from insect cells (Sf-9), coinfected with recombinant baculoviruses encoding three subunits (11 kDa, 34 kDa, and either wild-type or zinc-finger mutant 70 kDa). After the salt concentration (0.5 *M* NaCl) was adjusted, cell lysates were loaded onto a ssDNA cellulose column (1.0 × 8 cm) equilibrated with buffer A [25 m*M* Tris-HCl (pH 7.5), 10% glycerol, 0.02% Nonidet P-40, 1 m*M* dithiothreitol (DTT), 0.5 m*M* EDTA, 0.1 m*M* phenylmethylsulfonyl fluoride, 0.1 μg/ml leupeptin, and 0.2 μg/ml antipain] containing 0.5 *M* NaCl. The column was successively washed with 20 column volumes of buffer A containing 0.5 *M* NaCl and 0.8 *M* NaCl. The proteins were eluted with buffer A containing 2.0 *M* NaCl and 40% ethylene glycol. The eluted fractions were diluted fivefold with buffer A, and loaded onto an Affi-Gel Blue (Bio-Rad) column equilibrated with buffer A containing 0.5 *M* NaCl. After the column was washed with buffer A containing 0.5 *M* NaCl and 0.8 *M* NaCl, proteins were eluted with buffer containing 2.5 *M* NaCl and 40% ethylene glycol. The RPA-containing fractions were pooled and dialyzed against buffer A containing 50 m*M* NaCl and further purified on a Q-Sepharose column with a linear salt gradient (50 m*M* to 0.4 *M* NaCl). During purification, RPA was monitored by immunoblotting using anti-p70 and -p34 antibodies (25). Histidine-tagged XPA was prepared according to the procedure described previously (15).

Biomolecular interaction analysis

Interaction of wt-RPA , a zinc-finger mutant, and/or XPA with ssDNA (or UV-damaged DNA) was monitored using an SPR biosensor instrument, Biacore 3000 (Biacore) as described previously (27). For preparation of the biosensor surface with DNA, 5′-biotinylated 70mer DNA was diluted to 1.5 n*M* in a buffer containing 10 m*M* sodium acetate (pH 4.8) and 1.0 *M* NaCl, and manually injected onto an immobilized streptavidin surface of the Biacore sensor chip to the desired density in different flow cells. One flow cell was left underivatized to allow for refractive index change correction. Proteins were diluted in the running buffer containing 10 m*M* HEPES (pH 7.4), 150 m*M* NaCl, 2 m*M* $MgCl_2$, 0.005% polysorbate-20, and 1 m*M* DTT. Each experiment was repeated at least twice to assure reproducibility.

Electrophoretic mobility shift assay of RPA–ssDNA interaction

Oligo$(dT)_{50}$ was labeled with [γ-^{32}P]ATP (ICN) and T4 polynucleotide kinase (Roche Molecular Biochemical) based on the manufacturer's instructions. The indicated amount of wt-RPA or zinc-finger mutant was incubated with 100 fmol of 5′-^{32}P-labeled oligo$(dT)_{50}$ at room temperature for 25 min in a reaction mixture containing 50 m*M* HEPES-KOH (pH 7.8), poly(dI-dC) (0.2 μg), bovine serum albumin (0.2 μg/μl), 200 m*M* NaCl, and the indicated amounts of other chemicals. The RPA–ssDNA complex was analyzed on 5% polyacrylamide gels in 0.5X Tris–borate–EDTA buffer (acrylamide: bisacrylamide = 43.2:0.8). The gels were dried and exposed to x-ray films (Kodak). For quantification, the bands of interest were excised

from the gels and measured for radioactivity using a Beckman Scintillation Counter LS 6500.

Proteolytic analysis of wt-RPA and zinc-finger mutant with trypsin

The reaction mixture (60 μl) contained 0.1 *M* Tris-HCl (pH 8.5), 120 ng/μl wild-type or mutant RPA, and, where indicated, 200 ng/μl oligo(dT)$_{50}$. After the reaction mixture was incubated at room temperature for 15 min, 50 ng of trypsin (sequencing grade; Boehringer Mannheim) was added into the reaction. The reaction mixture was then immediately incubated at 37°C. Eight or 10 μl of the sample was removed from the reaction at the indicated time points. The reaction samples were separated by sodium dodecyl sulfate–polyacrylamide gel electrophoresis (SDS-PAGE) gel and were analyzed by the western blot (Fig. 1B).

Western blotting

Western blots were performed as described previously (25). In brief, wild-type or mutant RPA was run in a 12% SDS-PAGE gel and transferred to a nitrocellulose membrane (BA83; Bio-Rad). After the transfer, either anti-p70 or anti-p34 polyclonal antibody was used to detect RPA subunits, which were then revealed by ^{125}I-protein A (Amersham Corp.) treatment and visualized by autoradiography.

Circular dichroism (CD) analysis

CD spectra of purified wt-RPA and a zinc-finger mutant were acquired on a Jasco J-720 spectropolarimeter (Japan Spectroscopic Co.). Far-UV CD spectra (200–260 nm) were measured in a 1-mm path length quartz cell and represent averages of four accumulations with a protein concentration of 100 μg/ml in 25 m*M* Tris-HCl (pH 7.5), 10% (vol/vol) glycerol, 0.02% (vol/vol) NP40, 0.5 m*M* EDTA, 0.1 m*M* phenylmethylsulfonyl fluoride, 0.1 μg/m*M* leupeptin, 0.2 μg/ml antipain, and 200 m*M* NaCl. All spectra were baseline-corrected by subtraction of an averaged scan derived from the buffer alone to obtain the mean molar residue ellipticity (deg cm^2 dmol^{-1}). The result from CD spectra was deconvoluted to obtain information on the secondary structures that are mostly affected by the zinc-finger motif during interaction of protein with damaged DNA. The software program (CDnn) used to deconvolute CD spectra was obtained through the Internet (http://bioinformatik.biochemtech.uni-halle.de/cdnn/).

RESULTS

Role of zinc-finger motif in redox regulation: kinetic analysis of RPA's ssDNA binding activity

Our recent study indicates that all four zinc-finger cysteines are essential for redox regulation of RPA's–ssDNA binding activity (30). Redox regulation affects initial RPA-ssDNA interaction, but has no effect after RPA forms a stable complex with DNA (30), suggesting that the zinc-finger motif may mediate the initial interaction of RPA with ssDNA. To get an insight into the RPA–ssDNA interaction, we used the SPR technique to examine the ssDNA binding activity of wt-RPA and zinc-finger mutant (ZFM4) under various redox conditions, which allows macromolecular interactions to be measured in real time (27). wt-RPA or zinc-finger mutant ranging from 0.125 n*M* to 2 n*M* was injected onto a biosensor chip containing a low level (33 RU) of 70mer ssDNA for 600 s, followed by 900 s of a buffer injection period for dissociation. The sensorgram indicated that both wt-RPA and zinc-finger mutant bound to ssDNA with high affinity in the presence of 1 m*M* DTT (Fig. 2B and D). Under nonreducing conditions, however, wt-RPA exhibited very low ssDNA binding activity, whereas ZFM4 maintained its high-affinity binding to ssDNA (Fig. 2A and C, and Table 1). Interaction of wt-RPA with the ssDNA surface under nonreducing conditions was very weak, as indicated by the derived $K_D = 2.33 \times 10^{-8}$ *M*, 1/3,000th of the affinity observed for RPA under reducing conditions (Table 1). Even though wt-RPA exhibited a low-affinity binding to ssDNA under nonreducing conditions, it maintained a stable interaction with ssDNA once forming a complex.

A unique role for Zn(II) in RPA–ssDNA interaction

To understand the role of Zn(II) in the redox regulation of RPA–ssDNA interaction, we ex-

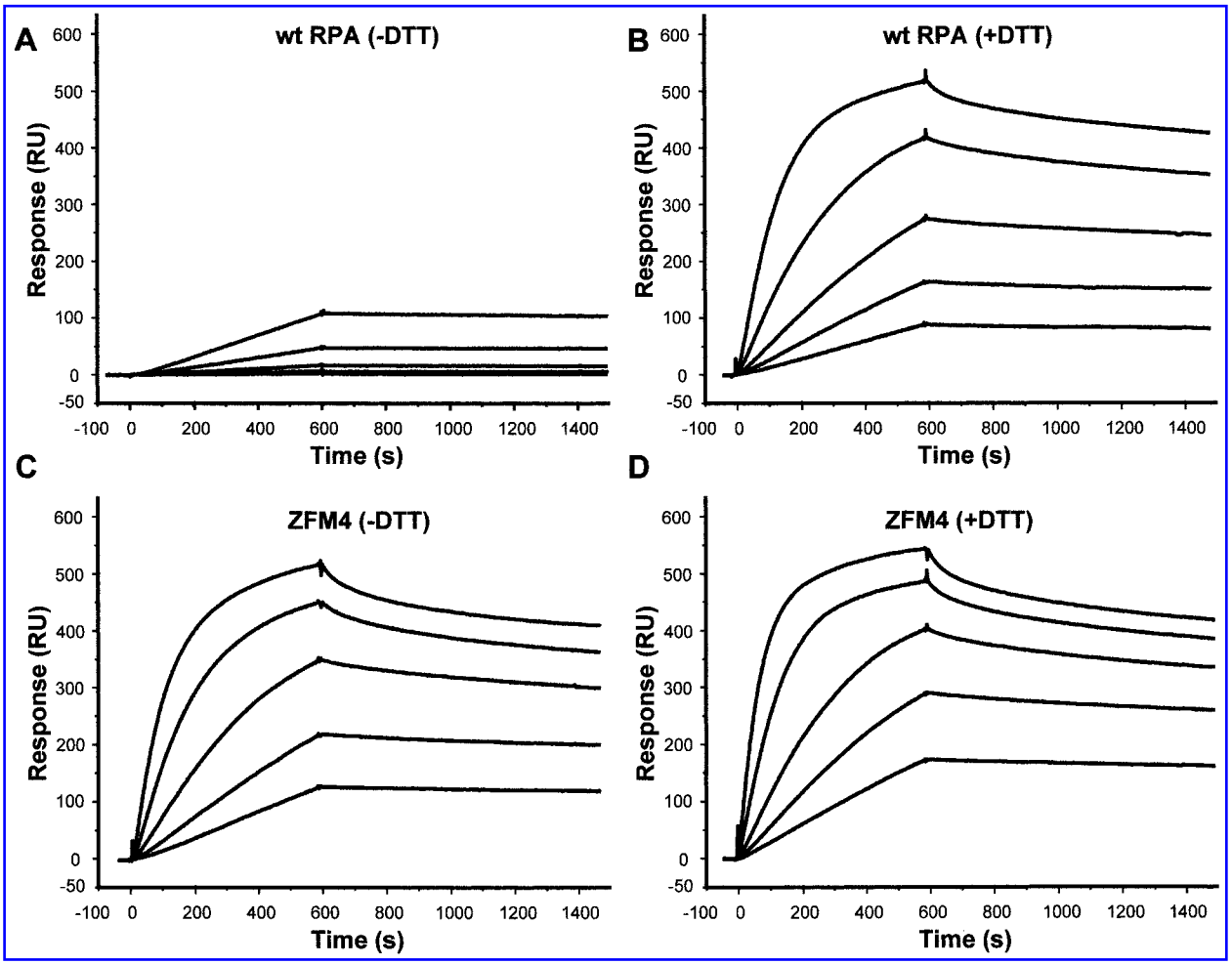

FIG. 2. Biomolecular interaction analysis of RPA–ssDNA binding under redox conditions. A 5 n*M* concentration of wt-RPA or a zinc-finger mutant (ZFM4) was injected onto a sensor chip surface containing 33 RU of ssDNA using the KINJECT function of Biacore 3000. The association phase was allowed for 600 s followed by 900 s of a buffer injection period for dissociation. (**A**) wt-RPA in the absence of DTT. (**B**) wt-RPA in the presence of 1 m*M* DTT. (**C**) ZFM4 in the absence of DTT. (**D**) ZFM4 in the presence of 1 m*M* DTT.

amined various divalent ions for RPA's ssDNA binding activity (Fig. 3). The role of Zn(II) in RPA-ssDNA interaction was supported by the fact that the inhibitory effect of the divalent ion chelator, *o*-phenanthroline, was reversed by addition of Zn(II) (30; Fig. 3A, lanes 4–6). In contrast, the interaction of the zinc-finger mutant with ssDNA was not affected by either *o*-phenanthroline or Zn(II) (Fig. 3A, lanes 7–16). Addition of an excess amount of Zn(II) nonspecifically inhibited RPA–ssDNA interaction regardless of *o*-phenanthroline's presence, suggesting that Zn(II)-dependent reversal of the inhibitory effect of *o*-phenanthroline functions within stoichiometric concentration (data not shown). To assess the role of Zn(II) in coordination of the zinc finger cysteine, we examined other divalent ions to see whether they can replace Zn(II) in RPA–ssDNA interaction (Fig. 3B). Mg(II), Ca(II), and Cu(II) were not able to compensate for Zn(II) in overcoming the inhibitory effect of *o*-phenanthroline in RPA–ssDNA interaction, whereas Fe(II) partially replaced Zn(II) (Fig. 3B). This result suggests that Zn(II) is the unique metal element coordinating four cysteine residues at RPA's zinc-finger motif.

Involvement of zinc-finger domain in RPA's structural change following interaction with DNA

To understand further the role of the zinc-finger motif in RPA–ssDNA interaction, we ex-

Table 1. Equilibrium and Kinetic Binding Constants of wt-RPA and a Zinc-Finger Mutant (ZFM4) to ssDNA

RPA	$K_D(M)$	$k_a(s^{-1}\ M^{-1})$	$k_d(s^{-1})$
+ DTT			
Wild-type	$(7.35 \pm 0.01) \times 10^{-11}$	$(2.76 \pm 0.02) \times 10^{-6}$	$(2.03 \pm 0.01) \times 10^{-4}$
ZFM4	$(4.47 \pm 0.04) \times 10^{-11}$	$(6.39 \pm 0.01) \times 10^{-6}$	$(2.86 \pm 0.02) \times 10^{-3}$
− DTT			
Wild-type	$(2.33 \pm 0.20) \times 10^{-8}$	$(2.38 \pm 0.06) \times 10^{-3}$	$(5.53 \pm 0.32) \times 10^{-5}$
ZFM4	$(4.97 \pm 0.03) \times 10^{-11}$	$(4.49 \pm 0.01) \times 10^{-6}$	$(2.23 \pm 0.01) \times 10^{-4}$

The data were globally fit to a 1:1 binding model.

amined far-UV CD spectra of wt-RPA and a zinc-finger mutant to see a change in secondary structure upon binding to DNA. A significant change in CD spectra was observed with both wt-RPA and a zinc-finger mutant upon binding to DNA (Fig. 4), suggesting that RPA undergoes a significant conformational change upon binding to DNA. A noticeable difference between wt-RPA and a zinc-finger mutant in the CD spectra pattern was observed under reducing conditions (Fig. 4A and C, and Table 2). Under nonreducing conditions, however, very little change in CD spectra between wt-RPA and zinc-finger mutant was observed (Fig. 4B and C, and Table 2). This result not only supports a role for the zinc-finger domain in the structural change of RPA, but also establishes a relationship between redox regulation and the structural change of RPA upon binding to DNA.

We also examined p70 and p34 subunits of wt-RPA and zinc-finger mutant for the tryptic digestion patterns in the presence and absence of ssDNA. In the absence of ssDNA, wt-RPA was cleaved into several tryptic products (55-, 47-, 19–21-, and 25-kDa fragments), whereas 19 kDa and 55 kDa were the major cleavage fragments in the presence of ssDNA (Fig. 5A). This result is in keeping with that from far-UV CD spectra analysis (Fig. 4) and suggests that RPA undergoes a conformational change upon binding to DNA (8, 21). The zinc-finger mutant, however showed very little change of its tryptic digestion in the presence of ssDNA (Fig. 5B), suggesting that a mutation at zinc-finger cysteine affects p70's conformational change upon binding to ssDNA. We also examined the tryptic digestion pattern of p34 to see whether the mutation at p70's zinc-finger domain affects the conformation of the p34 subunit. The p34 subunit of the zinc-finger mutant (ZFM4) was not only protected from tryptic digestion, but also unaffected by the presence of ssDNA (Fig. 5D). On the other hand, wt-RPA showed a change in the p34 tryptic digestion pattern upon binding to ssDNA, such that the p34 subunit was more accessible to tryptic digestion following RPA–ssDNA interaction. This result suggests that the mutation at the zinc-finger domain of p70 may also affect the accessibility of p34 to tryptic digestion.

Redox regulation of RPA's zinc-finger motif in recognition of damaged DNA

RPA not only has a preferential binding to UV- or cisplatin-damaged DNA, but also can stabilize XPA-damaged DNA complex through protein–protein interaction (2, 4, 22, 26, 27). Although zinc-finger mutant RPA failed to support NER activity (6), it also can stabilize the interaction of XPA with damaged DNA (26). We therefore examined whether redox affects RPA's interaction with damaged DNA and/or with XPA. Both XPA and wt-RPA are the 4-cysteine type zinc-finger proteins, and their interactions with UV-damaged DNA were affected by redox (Fig. 6A and B), whereas the interaction of the zinc-finger mutant RPA with damaged DNA was not affected by redox change (Fig. 6B). On the other hand, RPA's role in stabilization of XPA-damaged DNA complex was not affected by redox (Fig. 6A & 6B), suggesting that the failure of zinc-finger mutant in supporting NER may not be due to its role in interaction with damaged DNA or XPA. Redox regulation of the zinc finger significantly affected the initial RPA–ssDNA interaction, but

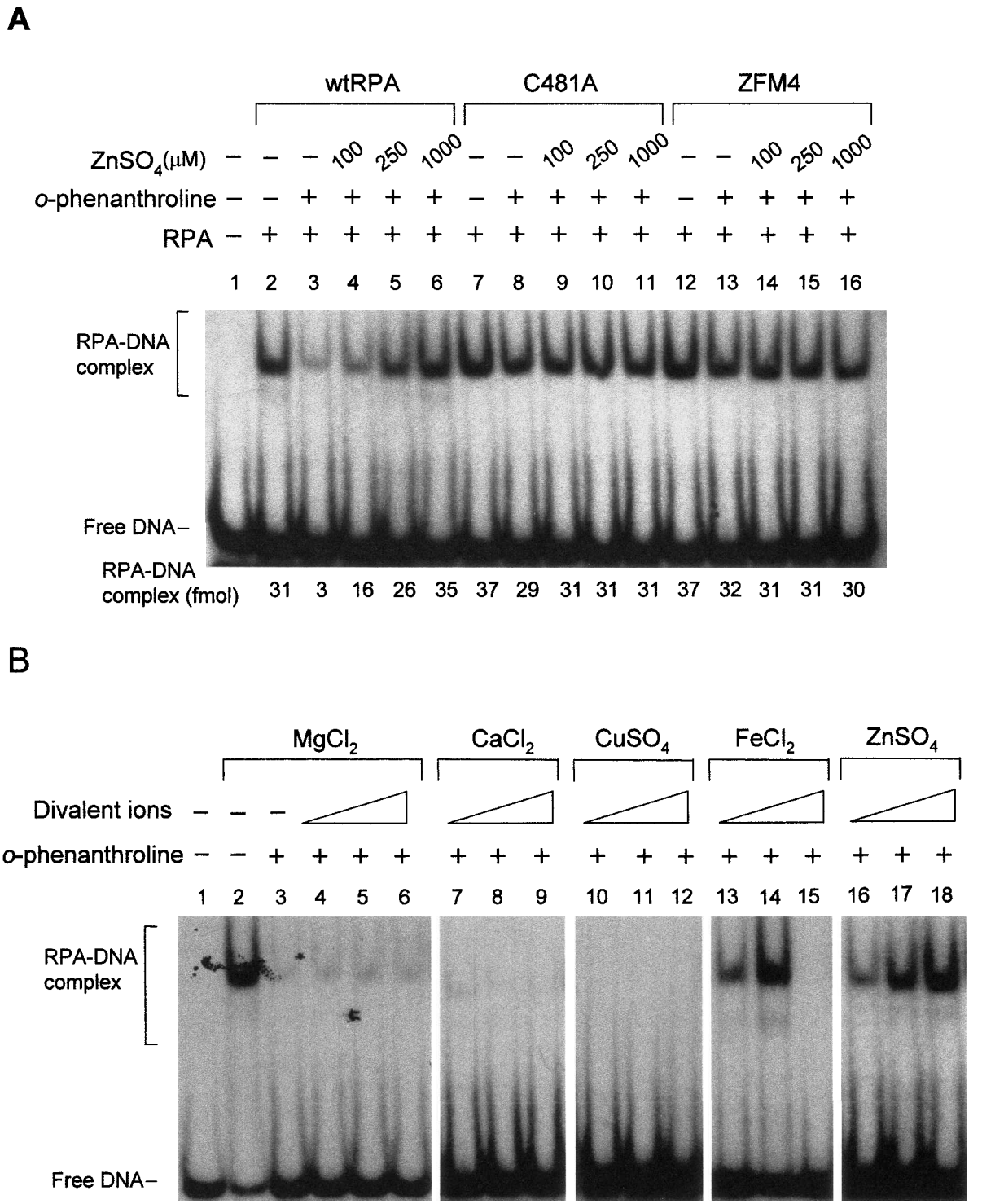

FIG. 3. (**A**) Inhibitory effect of *o*-phenanthroline on RPA ssDNA binding activity is restored by Zn(II). wt-RPA or zinc-finger mutant (20 ng) was treated with 1.0 m*M* *o*-phenanthroline followed by the addition of increasing amounts of Zn(II) to the reaction mixture. After incubation for 15 min in the presence of 100 fmol of 5′-^{32}P-labeled oligo(dT)$_{50}$, the RPA–ssDNA complex was analyzed by gel mobility shift assay (5% PAGE). Lane 1 contained no RPA. (**B**) Effect of various metal ions on RPA's ssDNA binding activity in the presence of *o*-phenanthroline. wt-RPA (20 ng) was treated with 1.0 m*M* *o*-phenanthroline and the indicated amounts of divalent metal (100 μM in lanes 4, 7, 10, 13, and 16; 250 μM in lanes 5, 8, 11, 14, and 17; 1,000 μM in lanes 6, 9, 12, 15, and 18) added to the reaction mixture before incubation for 15 min with 100 fmol of 5′-^{32}P-labeled oligo(dT)$_{50}$. No RPA was included in lane 1. The RPA–ssDNA complex was analyzed by the procedure as described in A.

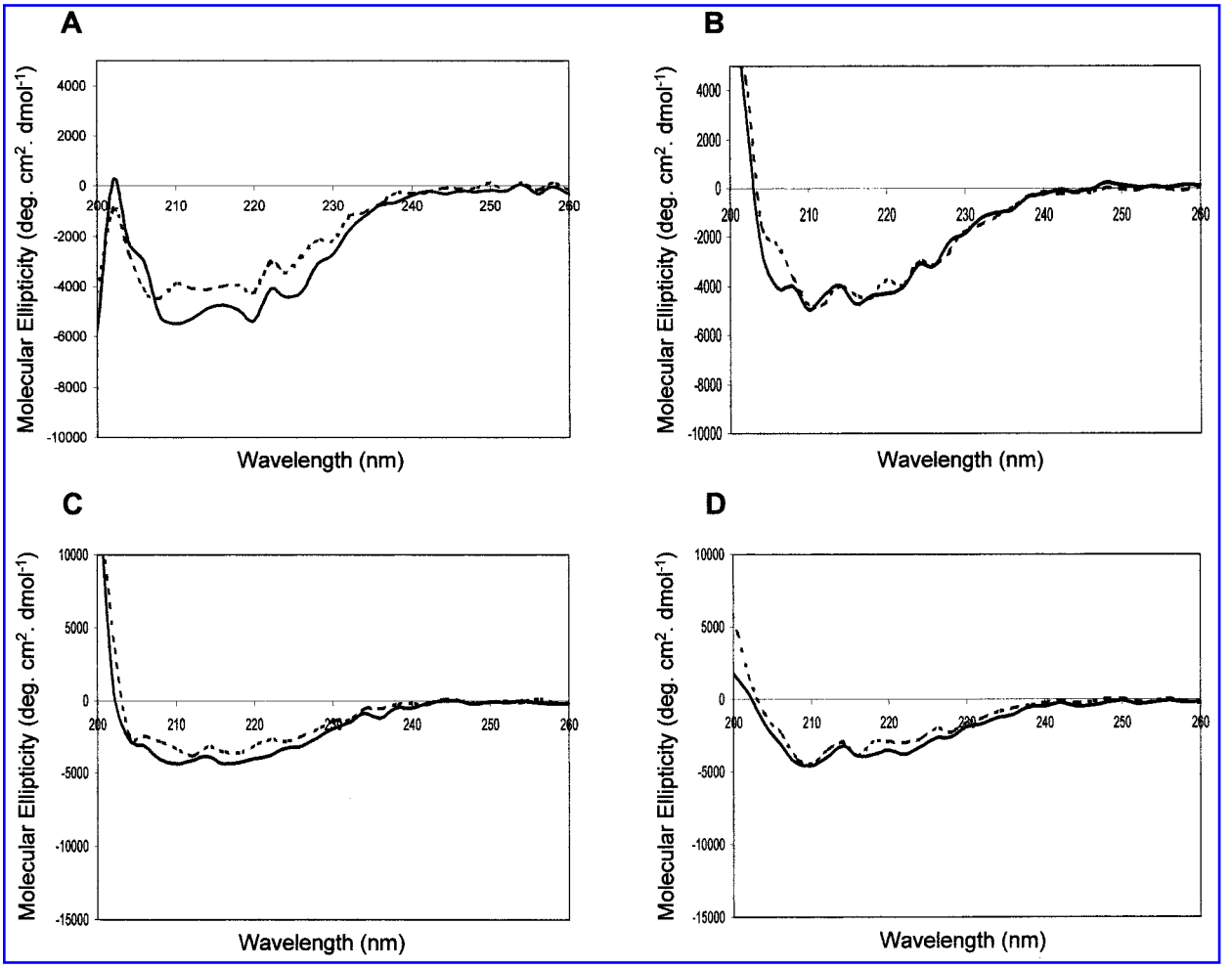

FIG. 4. Far-UV CD spectra of wild-type RPA (—) and zinc-finger mutant (ZFM4) (- - -) under various conditions. Reactions were carried out at 25°C in either the absence (**A** and **B**) or presence (**C** and **D**) of oligo(dT)$_{50}$. Reactions contained either 1 m*M* (**A** and **C**) or 0 m*M* DTT (**B** and **D**).

had no effect after RPA formed a stable complex with DNA (30). Similarly, RPA–XPA-damaged DNA complex, once formed, was not affected by redox (Fig. 6C), suggesting that the zinc-finger motif may mediate the transition of RPA–XPA interaction to a stable RPA–XPA-damaged DNA complex in a redox-dependent manner.

DISCUSSION

The zinc finger is one of the key structural motifs found in many DNA binding proteins in eukaryotes and implicates a role in the regulation of DNA binding activity through redox (9, 12, 29). Nonetheless, the role of the zinc finger in redox regulation has not been directly demonstrated because the zinc finger domain is essential for sequence-specific DNA binding and a mutation at this region would abolish DNA binding activity. RPA's zinc-finger motif is not a DNA binding element, and a mutation at the zinc-finger motif has very little effect on its DNA binding activity (8, 14, 16), which makes RPA an excellent model to study the role of zinc-finger motifs in redox regulation. In this study, we analyzed a role for RPA's zinc-finger motif in the redox regulation of RPA–DNA interaction.

The SPR analysis indicated that interaction of wt-RPA with ssDNA under nonreducing conditions was very weak and was only 1/3,000th of the affinity observed for RPA under reducing conditions (Table 1). Even though wt-RPA showed a low affinity to ssDNA un-

TABLE 2. FAR UV-CD ANALYSIS OF WT-RPA AND ZINC-FINGER MUTANT (ZFM)

	Helix (%)	*Antiparallel (%)*	*Parallel (%)*	*β-turn (%)*	*Random coil (%)*
wt-RPA (+ DTT)	10.9	29.6	5.5	20.3	36.1
wt-RPA (− DTT)	15.7	28.0	6.3	15.9	32.9
wt-RPA/DNA (+ DTT)	16.3	27.8	6.4	15.5	32.4
wt-RPA/DNA (− DTT)	11.4	31.1	5.8	18.5	35.0
ZFM (+ DTT)	9.9	31.4	5.4	20.3	36.3
ZFM (− DTT)	13.6	30.4	6.2	16.3	33.6
ZFM/DNA (+ DTT)	15.4	30.3	6.5	14.8	32.2
ZFM/DNA (− DTT)	11.7	32.3	6.0	17.4	34.4

der nonreducing conditions, it maintained a stable interaction with ssDNA once forming the RPA–ssDNA complex. This result is in keeping with a recent observation that redox regulation of the zinc finger significantly affected initial RPA–ssDNA interaction, but had no effect after RPA formed a stable complex with DNA (30). This result also suggests that

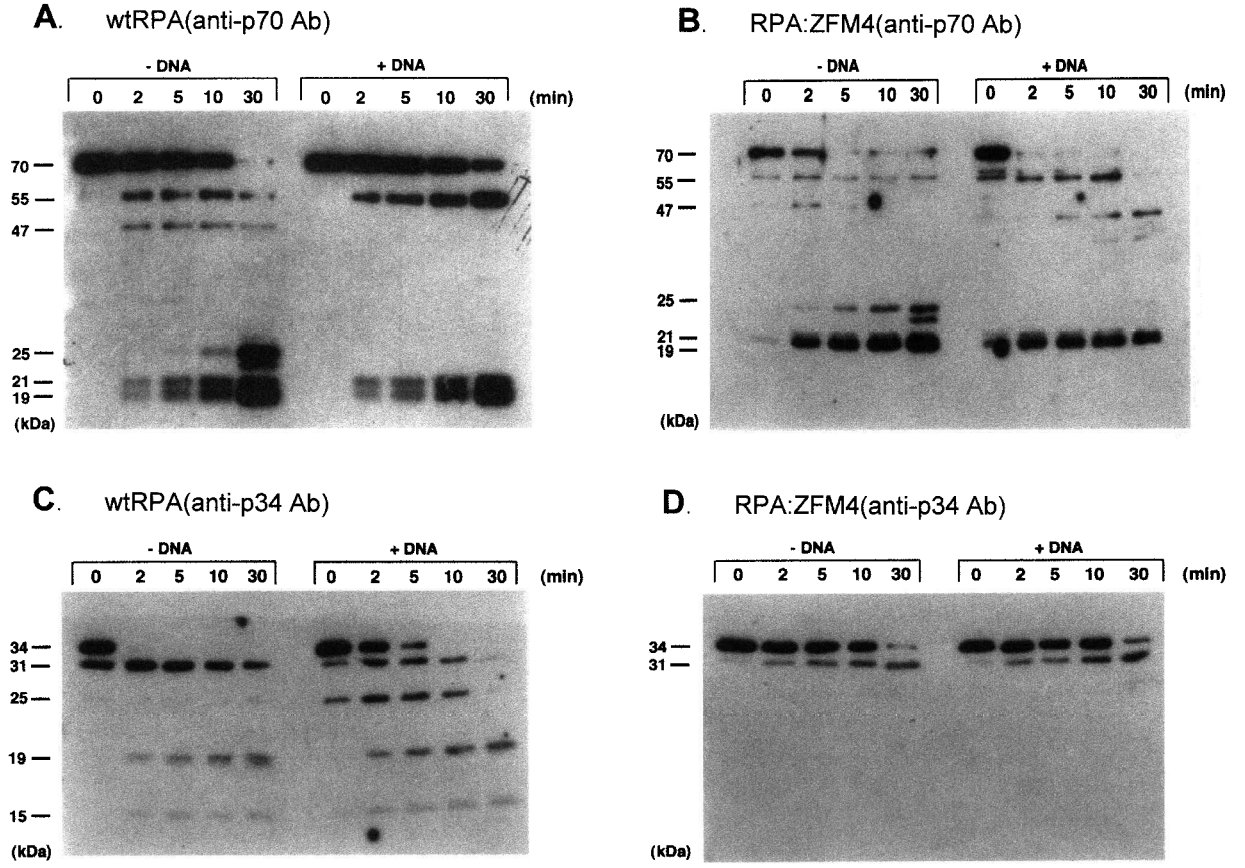

FIG. 5. Involvement of zinc-finger motif in the conformational change of RPA. (**A** and **B**) Tryptic digestion of RPA p70 subunit upon binding to ssDNA. Reaction mixtures (60 μl) contained 0.1 *M* Tris-HCl (pH 8.5) and 120 ng/μl of either wt-RPA (A) or a zinc-finger mutant (ZFM4) (B). Where indicated, 40 ng/μl oligo(dT) was added. After incubation at room temperature for 15 min, 50 ng of trypsin (sequencing grade; Boehringer Mannheim) was added to the reaction. Reaction mixtures were then incubated at 37°C, and aliquots were removed from the reactions at the indicated time points. Samples were mixed with gel loading buffer, boiled for 5 min, and loaded onto a 14% SDS-PAGE. The gel was then subjected to a western blot analysis using an anti-p70 polyclonal antibody. (**C** and **D**). Tryptic digestion pattern of RPA p34 subunit upon binding to ssDNA. Reaction mixtures and the sample preparations were the same as in A and B except that an anti-p34 polyclonal antibody was used to visualize p34 and its cleaved fragments for western analysis.

the zinc-finger motif mediates the transition of RPA–ssDNA interaction to a stable RPA–ssDNA complex in a redox-dependent manner.

The 4-cysteine zinc finger contains Zn(II) that tetrahedrally coordinates four cysteine residues (18). Under reducing conditions, the zinc-finger structure is favorably formed and Zn(II), buried in the interior, stabilizes the module by binding four cysteines (21), whereas the oxidation of the Zn(II)-thiolate bond induces the release of Zn(II) from the zinc finger, which likely promotes disulfide bond formation between the zinc-finger cysteines (21, 30). Other divalent ions were not able to compensate for Zn(II) in overcoming the inhibitory effect of *o*-phenanthroline in RPA–ssDNA interaction (Fig. 3), suggesting that Zn(II) may play a unique role in coordinating the zinc finger cysteines, which in turn controls RPA's ssDNA binding activity. The latter is also supported by the fact that a mutation at zinc-finger cysteines (amino acids 481, 486, 500, or 503) would be sufficient to abolish redox sensitivity of RPA's ssDNA binding activity (21, 30).

A significant change in the tryptic digestion pattern observed with wt-RPA, but not with a zinc-finger mutant, upon binding to ssDNA (Fig. 5A) strongly suggests that the conformational change of p70 occurs in an ssDNA-dependent manner, which mainly protects the large domain of p70 (55-kDa fragment) from proteolytic digestion. One possibility is that the 55-kDa fragment may actually be involved in the conformational change of p70 and protected from tryptic digestion through its interaction with ssDNA. It would be interesting to see whether the protected region of p70 (55-kDa fragment) represents the domain directly in contact with ssDNA. The p34 subunit (wt-RPA) also showed a change in the tryptic digestion pattern, becoming more accessible to tryptic digestion following its interaction with ssDNA, whereas the tryptic digestion pattern of the p34 subunit from the zinc-finger mutant (ZFM4) was virtually unaffected by the presence of ssDNA (Fig. 5D). This result suggests that the zinc-finger domain of p70 not only is essential for the conformational change of its own subunit, but may also affect the accessibility of p34 to tryptic digestion. The latter possibility was also supported by the previous finding where DNA-dependent protein kinase phosphorylated the p34 subunit from wt-RPA, but not that from the zinc-finger mutant, in the presence of ssDNA (6).

A role for RPA's zinc-finger domain has been demonstrated previously indicating that mutations at the zinc-finger domain differentially affected its function in DNA replication and NER (6, 17). The failure of zinc-finger mutants in supporting NER was not due to its role in the stabilization of the XPA-damaged DNA complex (26, 27). It is possible that the zinc-finger motif may be involved in mediating the generation of ssDNA during RPA-damaged DNA interaction (23). No matter what the role of RPA's zinc-finger domain in DNA repair may be, the initial interaction of XPA with damaged DNA under nonreducing conditions was significantly affected in the presence of wt-RPA, but not in the presence of a zinc-finger mutant (Fig. 6). It is not clear whether the differential effect of wt-RPA and a zinc-finger mutant on the XPA-damaged DNA interaction plays a direct role in NER. Considering the fact that the zinc-finger domain is involved in the conformational change of the RPA p70 subunit, it is conceivable that RPA's zinc-finger domain and its redox regulation may affect the early stage of repair, such as formation of a damage-recognition complex.

FIG. 6. Biacore analysis of redox regulation of RPA stabilization of XPA–(64) photoproduct interaction. wt-RPA or ZFM4 was injected onto a sensor chip surface containing 2,000 RU of double-stranded DNA, which contains a centrally located (6–4) photoproduct, using the KINJECT function of Biacore 3000. The association phase was allowed for 300 s followed by 540 s of a buffer injection period for dissociation. (**A**) wt-RPA (1 n*M*), XPA (2.5 n*M*), and the mixture of XPA (2.5 n*M*) and wt-RPA (1 n*M*) in the presence (1 m*M*) and absence of DTT. (**B**) ZFM4 RPA (1 n*M*), XPA (2.5 n*M*), and the mixture of XPA (2.5 n*M*) and ZFM4 RPA (1 n*M*) in the presence (1 m*M*) and absence of DTT. (**C**) wt-RPA (1 n*M*), XPA (2.5 n*M*), and the mixture of XPA (2.5 n*M*) and wt-RPA (1 n*M*) were injected onto the sensor chip surface in the presence of 1 m*M* DTT for a period of 300 s for association followed by a dissociation of 540 s by washing with a buffer containing either 1 m*M* or 0 m*M* DTT.

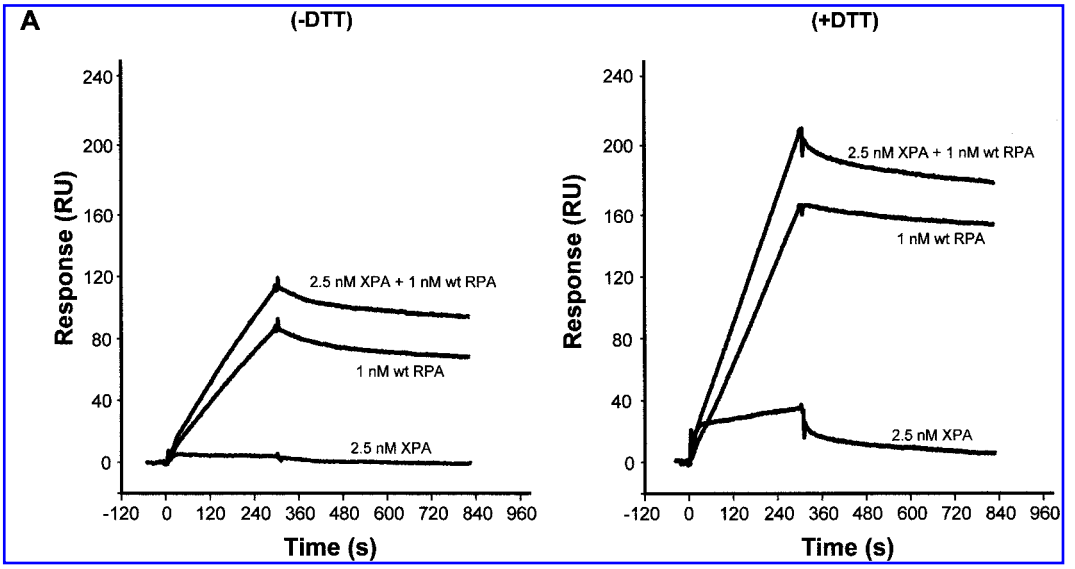
A
(-DTT)
(+DTT)
Response (RU)
Time (s)
2.5 nM XPA + 1 nM wt RPA
1 nM wt RPA
2.5 nM XPA

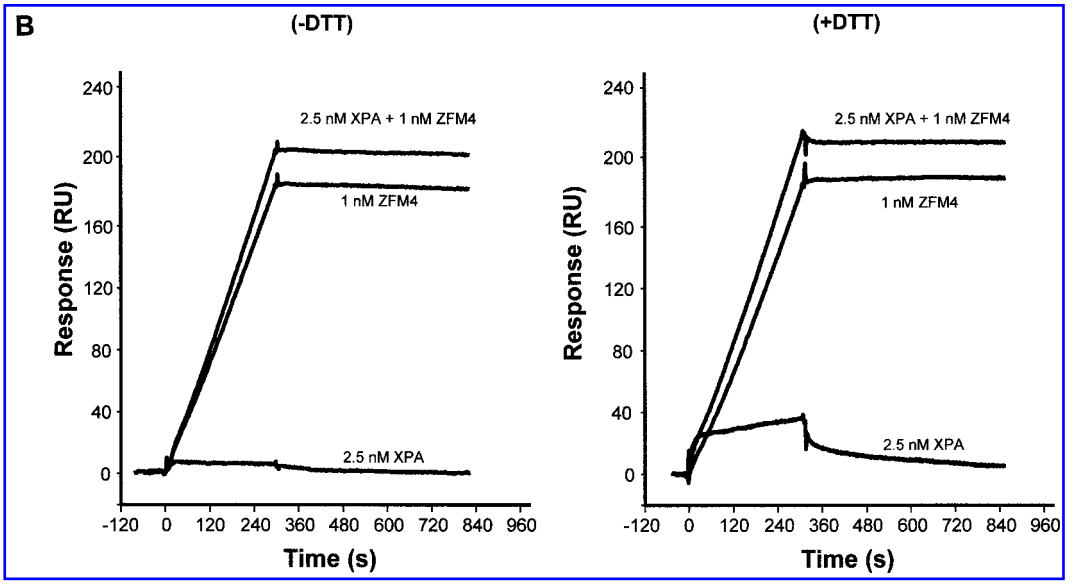
B
(-DTT)
(+DTT)
Response (RU)
Time (s)
2.5 nM XPA + 1 nM ZFM4
1 nM ZFM4
2.5 nM XPA

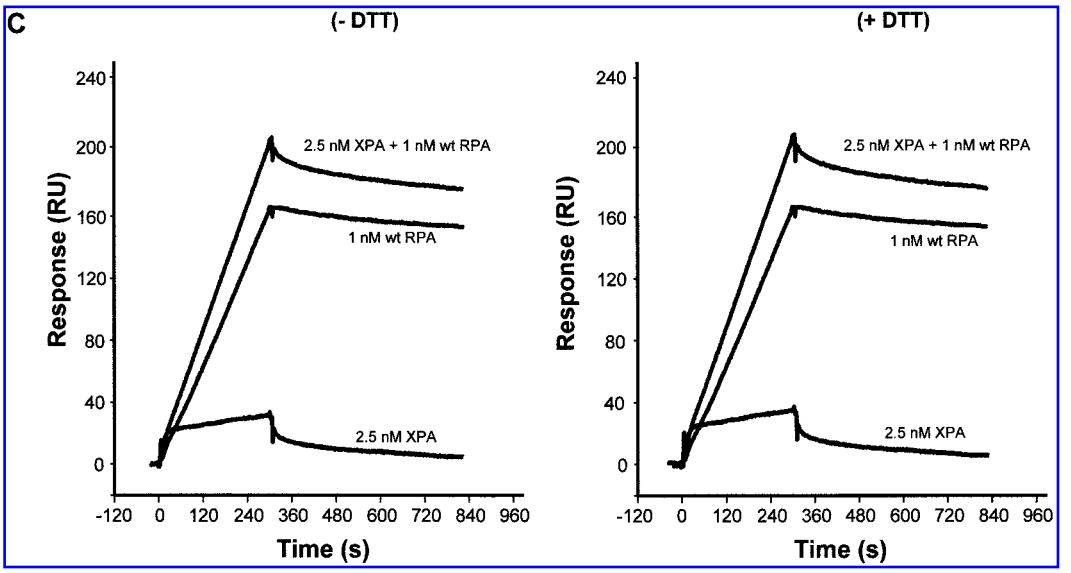
C
(- DTT)
(+ DTT)
Response (RU)
Time (s)
2.5 nM XPA + 1 nM wt RPA
1 nM wt RPA
2.5 nM XPA

ACKNOWLEDGMENTS

We would like to thank Dr. John Hawes for help with HPLC purification of oligonucleotides containing DNA damage, and Dr. Alan Mahrenholz for valuable suggestions throughout the course of this study. This research was supported by grants from the U.S. Army (DAMD17-00-1-0295), NIH (CA92111), and the Catherine Peachey Funds. M.W. was supported by a postdoctoral fellowship from NIH (F32 GM20167-01).

ABBREVIATIONS

CD, circular dichroism; DTT, dithiothreitol; ERCC1, excision repair cross complementing protein 1; NER, nucleotide excision repair; RPA, replication protein A; SDS-PAGE, sodium dodecyl sulfate–polyacrylamide gel electrophoresis; SPR, surface plasmon resonance; ssDNA, single-stranded DNA; TFIIH, transcription factor IIH; UV, ultraviolet ray; wt-RPA, wild-type RPA; XPA, xeroderma pigmentosum group A protein; ZFM, zinc-finger mutant RPA.

REFERENCES

1. Aboussekhra A, Biggerstaff M, Shivji MK, Vilpo JA, Moncollin V, Podust VN, Protic M, Hubscher U, Egly JM, and Wood RD. Mammalian DNA nucleotide excision repair reconstituted with purified protein components. *Cell* 80: 859–868, 1995.
2. Batty DP and Wood RD. Damage recognition in nucleotide excision repair of DNA. *Gene* 241: 193–204, 2000.
3. Bochkarev A, Pfuetzner RA, Edwards AM, and Frappier L. Structure of the single-stranded DNA-binding domain of replication protein A bound to DNA. *Nature* 385: 176–181, 1997.
4. Burns JL, Guzder SN, Sung P, Prakash S, and Prakash L. An affinity of human replication protein A for ultraviolet-damaged DNA. Implications for damage recognition in nucleotide excision repair. *J Biol Chem* 271: 11607–11160, 1996.
5. Collins KL and Kelly TJ. Effects of T antigen and replication protein A on the initiation of DNA synthesis by DNA polymerase α-primase. *Mol Cell Biol* 11: 2108–2115, 1991.
6. Dong J, Park JS, and Lee SH. In vitro analysis of the zinc-finger motif in human replication protein A. *Biochem J* 337: 311–317, 1999.
7. Dornreiter I, Erdile LF, Gilbert IU, von Winkler D, Kelly TJ, and Fanning E. Interaction of DNA polymerase alpha-primase with cellular replication protein A and SV40 T antigen. *EMBO J* 11: 769–776, 1992.
8. Gomes XV and Wold MS. Functional domains of the 70–kilodalton subunit of human replication protein A. *Biochemistry* 35: 10558–10568, 1996.
9. Gowen LC, Avrutskaya AV, Latour AM, Koller BH, and Leadon SA. BRCA1 required for transcription-coupled repair of oxidative DNA damage. *Science* 281: 1009–1012, 1998.
10. Guzder SN, Sung P, Prakash L, and Prakash S. Yeast DNA-repair gene RAD14 encodes a zinc metalloprotein with affinity for ultraviolet-damaged DNA. *Proc Natl Acad Sci U S A* 90: 5433–5437, 1993.
11. He Z, Henricksen LA, Wold MS, and Ingles CJ. RPA involvement in the damage-recognition and incision steps of nucleotide excision repair. *Nature* 374: 566–569, 1995.
12. Hutchison KA, Matic G, Meshinchi S, Bresnick EH, and Pratt WB. Redox manipulation of DNA binding activity and BuGR epitope reactivity of the glucocorticoid receptor. *J Biol Chem* 266: 10505–10509, 1991.
13. Jones CJ and Wood RD. Preferential binding of the xeroderma pigmentosum group A complementing protein to damaged DNA. *Biochemistry* 32: 12096–12104, 1993.
14. Kim DK, Stigger E, and Lee SH. Role of the 70–kDa subunit of human replication protein A (I). Single-stranded DNA binding activity, but not polymerase stimulatory activity, is required for DNA replication. *J Biol Chem* 271: 15124–15129, 1996.
15. Lee SH and Kim DK. The role of the 34–kDa subunit of human replication protein A in simian virus 40 DNA replication in vitro. *J Biol Chem* 270: 12801–12807, 1995.
16. Lin YL, Chen C, Keshav KF, Winchester E, and Dutta A. Dissection of functional domains of the human DNA replication protein complex replication protein A. *J Biol Chem* 271: 17190–17198, 1996.
17. Lin YL, Shivji MKK, Chen C, Kolodner R, Wood RD, and Dutta A. The evolutionarily conserved zinc finger motif in the largest subunit of human replication protein A is required for DNA replication and mismatch repair but not for nucleotide excision repair. *J Biol Chem* 273: 1453–1461, 1998.
18. Luisi BF, Xu WX, Otwinowski Z, Freedman LP, Yamamoto KR, and Sigler PB. Crystallographic analysis of the interaction of the glucocorticoid receptor with DNA. *Nature* 352: 497–505, 1991.
19. Matsunaga T, Park CH, Bessho T, Mu D, and Sancar A. Replication protein A confers structure-specific endonuclease activities to the XPF-ERCC1 and XPG subunits of human DNA repair excision nuclease. *J Biol Chem* 271: 11047–11050, 1996.
20. Melendy T and Stillman B. An interaction between replication protein A and SV40 T antigen appears es-

sential for primosome assembly during SV40 DNA replication. *J Biol Chem* 268: 3389–3395, 1993.
21. Park JS, Wang M, Park SJ, and Lee SH. Zinc finger of replication protein A, a non-DNA binding element, regulates its DNA binding activity through redox. *J Biol Chem* 274: 29075–29080, 1999.
22. Patrick SM and Turchi JJ. Human replication protein A preferentially binds cisplatin-damaged duplex DNA in vitro. *Biochemistry* 37: 8808–8815, 1998.
23. Patrick SM and Turchi JJ. Replication protein A (RPA) binding to duplex cisplatin damaged DNA is mediated through the generation of single-stranded DNA. *J Biol Chem* 274: 14972–14978, 1999
24. Robins P, Jones CJ, Biggerstaff M, Lindahl T, and Wood RD. Complementation of DNA repair in xeroderma pigmentosum group A cell extracts by a protein with affinity for damaged DNA. *EMBO J* 10: 3913–3921, 1991.
25. Stigger E, Dean FB, Hurwitz J, and Lee SH. Reconstitution of functional human single-stranded DNA-binding protein from individual subunits expressed by recombinant baculoviruses. *Proc Natl Acad Sci U S A* 91: 579–583, 1994.
26. Stigger E, Drissi R, and Lee SH. Functional analysis of human replication protein A in nucleotide excision repair. *J Biol Chem* 273: 9337–9343, 1998.
27. Wang M, Mahrenholz A, and Lee SH. RPA stabilizes the XPA-damaged DNA complex through protein–protein interaction. *Biochemistry* 39: 6433–6439, 2000.
28. Wold MS. Replication protein A: a heterotrimeric, single-stranded DNA-binding protein required for eukaryotic DNA metabolism. *Annu Rev Biochem* 66: 61–92, 1997.
29. Wu X, Bishopric NH, Discher DJ, Murphy BJ, and Webster KA. Physical and functional sensitivity of zinc finger transcription factors to redox change. *Mol Cell Biol* 16: 1035–1046, 1996.
30. You JS, Wang M, and Lee SH. Functional characterization of zinc-finger motif in redox regulation of RPA–ssDNA interaction. *Biochemistry* 39: 12953–12958, 2000.

Address reprint requests to:
Dr. S.-H. Lee
Department of Biochemistry and Molecular Biology
Indiana University School of Medicine
635 Barnhill Dr.
Indianapolis, IN 46202

E-mail: slee@iupui.edu

Received for publication November 2, 2000; accepted January 28, 2001.

This article has been cited by:

1. Joseph Shlomai . 2010. Redox Control of Protein–DNA Interactions: From Molecular Mechanisms to Significance in Signal Transduction, Gene Expression, and DNA ReplicationRedox Control of Protein–DNA Interactions: From Molecular Mechanisms to Significance in Signal Transduction, Gene Expression, and DNA Replication. *Antioxidants & Redox Signaling* **13**:9, 1429-1476. [Abstract] [Full Text] [PDF] [PDF Plus]
2. Rebecca L. Rich, David G. Myszka. 2002. Survey of the year 2001 commercial optical biosensor literature. *Journal of Molecular Recognition* **15**:6, 352-376. [CrossRef]